[8] Morkovin, M. V., "Critical Evaluation of Transition From Laminar to Turbulent Shear Layers with Emphasis on Hypersonically Traveling Bodies," AFFDL-TR-68-149, March 1969, Air Force Flight Dynamics Lab., Wright-Patterson Air Force Base.

[9] Potter, J. L. and Whitfield, J. P., "Boundary Layer Transition under Hypersonic Conditions," AGARDograph 97, Pt. 3, 1965.

[10] Beckwith, I. E. and Cohen, N. B., "Application of Similar Solutions to Calculation of Laminar Heat Transfer on Bodies with Yaw and Large Pressure Gradient in High-Speed Flow," TN D-625, 1960, NASA.

[11] Henderson, A., Jr., Rogallo, R. S., Woods, W. C., and Spitzer, C. R., "Exploratory Hypersonic Boundary-Layer Transition Studies," *AIAA Journal*, Vol. 3, No. 7, July 1965, pp. 1363–1364.

[12] Staylor, W. F. and Morrisette, E. L., "Use of Moderate-Length Hot Wires to Survey a Hypersonic Boundary Layer," *AIAA Journal*, Vol. 5, No. 9, Sept. 1967, pp. 1698–1700.

[13] Stainback, P. C., "Use of Rouse's Stability Parameter in Determining the Critical Layer Height of a Laminar Boundary Layer," *AIAA Journal*, Vol. 8, No. 1, Jan. 1970, pp. 173–175.

[14] Harris, J. E., "Numerical Solution of the Equations for Compressible Laminar, Transitional, and Turbulent Boundary Layers and Comparisons with Experimental Data," TR R-368, Aug. 1971, NASA.

[15] Adams, J. C., Jr., "Eddy Viscosity-Intermittency Factor Approach to Numerical Calculation of Transitional Heating on Sharp Cones in Hypersonic Flow," AEDC-TR-70-210, Nov. 1970, Arnold Engineering Development Center, Arnold Air Force Station, Tenn.

Cross-Hatching as an Aeroviscoelastic Problem

EARL H. DOWELL*
Princeton University, Princeton, N.J.

PROBSTEIN and Gold[1] have recently given an analysis of the phenomena of "cross-hatching," i.e., the formation of diamond-shaped patterns on the surface of bodies exposed to a supersonic flow. In their theoretical model, the cross-hatching results from the instability of a coupled fluid-(viscoelastic) solid interaction, hence one might term it an "aeroviscoelastic" problem. Whatever one calls it, the considerable experience developed in the field of aeroelasticity may be used to gain further insight into their model and its possible relevance to cross-hatching. In particular, we shall use the methods and to some extent the results of Ref. 2 and references cited therein to assess the Probstein-Gold model.

Analysis of Probstein-Gold Model

An inviscid, potential flow model is employed where the perturbation pressure p' satisfies (the notation is that of Ref. 1)

$$(1-M^2)\partial^2 p'/\partial x^2+\partial^2 p'/\partial y^2=(M^2/U^2)(\partial/\partial t)(\partial p'/\partial t+2U\,\partial p'/\partial x) \tag{1}$$

The boundary condition at the fluid-solid interface is

$$\rho(D^2\delta/Dt^2)=-\partial p'/\partial y|_{y=0} \tag{2}$$

where δ is the vertical solid displacement. The equation of motion of the viscoelastic solid is taken to be

$$\tau(D/Dt)\partial\delta/\partial x=\kappa p'-\partial\delta/\partial x \tag{3}$$

We examine traveling wave solutions which assumes the finite dimensions of the solid are, in some sense, unimportant.

Assume

$$\delta=\bar{\delta}\,e^{i\omega t+i\alpha x};\quad p'=\bar{p}\,e^{i\omega t+i\alpha x}$$

From Eq. (1)

$$(i\alpha)^2[1-M^2(1+i\omega/Ui\alpha)^2]\bar{p}+d^2\bar{p}/dy^2=0$$

The two independent solutions are

$$\bar{p}=e^{\pm i\alpha[M^2(1+i\omega/Ui\alpha)^2-1]^{1/2}y} \tag{4}$$

We shall select the minus sign to satisfy the Sommerfeld condition. (This point is actually more subtle, see Ref. 2 and references cited therein.) From Eq. (2)

$$\rho(i\omega+Ui\alpha)^2\bar{\delta}=-\partial\bar{p}/\partial y|_0$$

From Eq. (3)

$$i\alpha[\tau(i\omega+Ui\alpha)+1]\bar{\delta}=\kappa\bar{p}$$

Combining the above two equations

$$\rho(i\omega+Ui\alpha)^2\kappa\bar{p}/i\alpha[\tau(i\omega+Ui\alpha)+1]=-\partial\bar{p}/\partial y|_{y=0} \tag{5}$$

Using Eq. (4) in Eq. (5) and cancelling out common factors

$$\rho(i\omega+Ui\alpha)^2\kappa/i\alpha[\tau(i\omega+Ui\alpha)+1]=i\alpha[M^2(1+i\omega/Ui\alpha)^2-1]^{1/2} \tag{6}$$

This is the eigenvalue equation to determine the permissible values of ω. Equation (6) is not given explicitly in Ref. 1, but presumably was obtained by Probstein-Gold.

At this point the authors of Ref. 1 assumed the instability was a static one (presumably based upon experimental observations) and assumed consequently that ω was a purely imaginary number. They then sought solutions of maximum growth rate as a function of the problem parameters from Eq. (6) or their equivalent of same. We shall return to their approach later but for the moment shall pursue a different approach.

Introduce nondimensional variables and parameters as follows:

$$\Omega\equiv i\omega/Ui\alpha,\quad \tau U\alpha\equiv\varepsilon^*,\quad \rho U^2\kappa\equiv\lambda^*$$

From Eq. (6)

$$\lambda^*[\Omega+1]^2/[i\varepsilon^*(\Omega+1)+1]=[M^2(1+\Omega)^2-1]^{1/2} \tag{7}$$

Hence, we see that

$$\Omega=\Omega(\lambda^*,M,\varepsilon^*)$$

Further define

$$\lambda\equiv\lambda^*/M^2$$
$$X\equiv M(1+\Omega)$$
$$\varepsilon\equiv\varepsilon^*/M$$

then Eq. (7) may be written even more compactly

$$E\equiv\lambda X^2/[i\varepsilon X+1]=(X^2-1)^{1/2}\equiv F \tag{8}$$

and hence, $X=X(\lambda,\varepsilon)$.

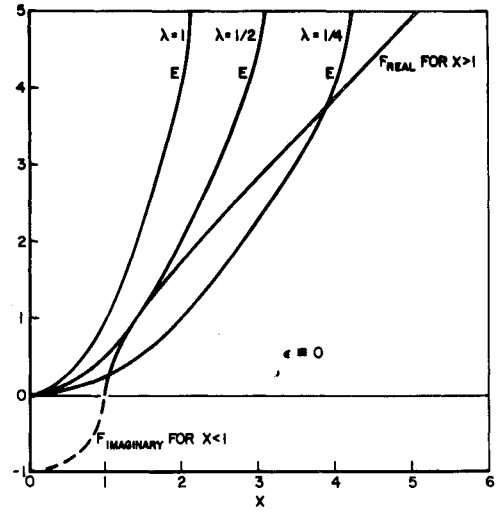

Fig. 1 Graphical solution to eigenvalue equation.

Received September 30, 1971; revision received December 17, 1971. The author would like to thank the reviewer for a number of helpful comments.

Index categories: Supersonic and Hypersonic Flow; Aeroelasticity and Hydroelasticity.

* Department of Aerospace and Mechanical Sciences. Member AIAA.

Special Case: $\varepsilon \equiv 0$ [A Purely Elastic Material with No Dissipation (Damping)]

For this type of equation it is known[2,3] that the eigenvalues are purely real until they coalesce at some critical value of λ, say $\lambda = \lambda_f$. For $\lambda > \lambda_f$ the eigenvalues become complex and at least one eigenfrequency or pole is unstable.

At the coalescence condition (i.e., the flutter condition)

$$E = F; \quad dE/dX = dF/dX \tag{9}$$

From the preceding one may determine that

$$\lambda_f = \tfrac{1}{2} \quad \text{and} \quad X_f^2 = 2$$

Hence,

$$\lambda_f^* = M^2/2 \tag{10}$$

and

$$\Omega_f = (2)^{1/2}/M - 1 \tag{11}$$

Note there is no preferred wavelength or wavenumber for the instability as α appears in Ω_f but not in λ_f^*, i.e., no particular choice of α minimizes λ_f^*. Also it is seen that at $M^2 = 2$ the instability is a static one, $\Omega_f = 0$. For $M^2 > 2$ the waves travel downstream and for $M^2 < 2$ they travel upstream. To make these results clearer, in Fig. 1 we present graphs of $E(X)$, $F(X)$.

It is seen that as $\lambda \to 0$, there are two (four) frequencies, $X = +1, +\infty(-1, -\infty)$. As λ increases these two frequencies come together. For $\lambda > \frac{1}{2}$ the frequencies are complex (no solutions for real X are possible) and the material is dynamically unstable (flutters).

Note: $|X| > 1$ and $X^2 = 2$ in particular means that flow is always effectively supersonic. Hence, the previous choice of aerodynamic branch in Eq. (4) is justified.

Now let us consider the viscous nature of the material. Since ε is apt to be small we use a convenient method which takes advantage of this fact.

Perturbation Analysis for Small ε

Let $X = X_0 + X_1\varepsilon$, then from Eq. (8) (retaining terms to order ε)

$$\begin{aligned}&\lambda(X_0^2 + 2X_1X_0\varepsilon + \ldots)\\ &= (X_0^2 + 2X_0X_1\varepsilon - 1)^{1/2}(1 + iX_0\varepsilon + \ldots)\\ &= (X_0^2-1)^{1/2}[1 + X_0X_1\varepsilon/(X_0^2-1) + \ldots](1 + iX_0\varepsilon + \ldots)\end{aligned} \tag{12}$$

Equating coefficients of same order

$$\varepsilon^0: \lambda X_0^2 = (X_0^2-1)^{1/2} \tag{13}$$

$$\varepsilon^1: 2\lambda X_0X_1 = (X_0^2-1)^{1/2}[X_0X_1/(X_0^2-1) + iX_0] \tag{14}$$

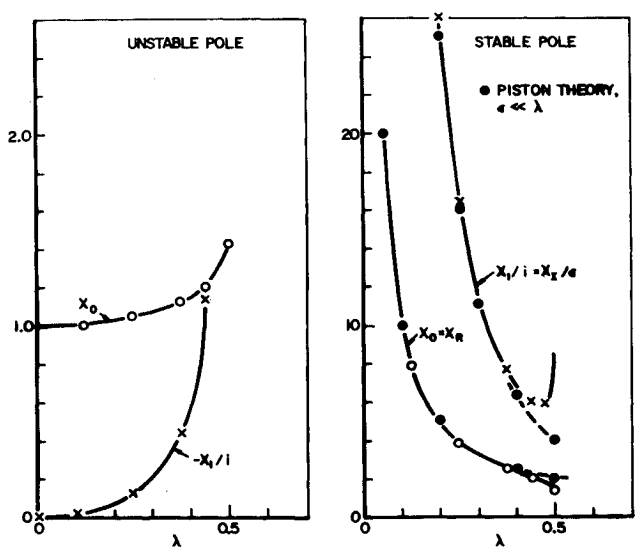

Fig. 2 Root loci.

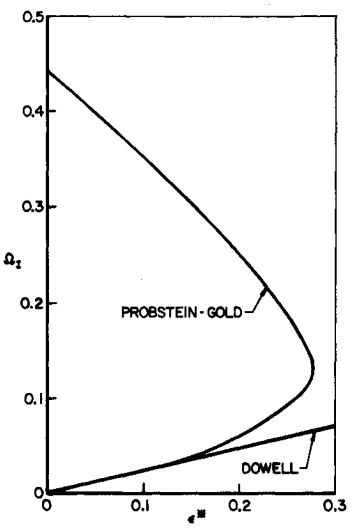

Fig. 3 Comparison of two analyses.

Dividing Eq. (14) by Eq. (13, and rearranging, one obtains

$$X_1 = iX_0^2(X_0^2-1)/(X_0^2-2)$$

Note that $X_0 = X_0(\lambda)$; also $X_0^2 > 1$ for all $\lambda \geqq \frac{1}{2}$. However, X_0^2 can be greater or less than 2. For the pole which is $X_0 = +\infty(-\infty)$ at $\lambda = 0$, X_0^2 is always greater than 2 up until $\lambda = \frac{1}{2}$. Conversely, for the pole which begins at $X_0 = +1(-1)$, X_0^2 is always less than 2 up until $\lambda = \frac{1}{2}$. Recall that

$$\begin{aligned}p, \delta \sim e^{i\omega t} &\sim e^{i\Omega_I U\alpha}\\ &\sim e^{-X_I tU\alpha}\\ &\sim e^{-\varepsilon tU\alpha X_0^2(X_0^2-1)/(X_0^2-2)}\end{aligned}$$

Thus, $X_0^2 < 2$ represents a growing motion and $X_0^2 > 2$ a decaying one. Hence, any pole is always stable or unstable with no nontrivial neutrally stable solutions possible for $\lambda > 0$ and $\varepsilon > 0$. For $\lambda \ll \frac{1}{2}$ and $X_0 \to +1, \infty$ the stable pole is highly damped and the unstable pole is only mildly unstable. However, strictly speaking, the model is always unstable for $\lambda > 0$ and $\varepsilon > 0$.

In Fig. 2 root loci of the poles are plotted. Note that the small ε expansion breaks down as $\lambda \to \frac{1}{2}$, $X_0^2 \to 2$ indicating one pole is becoming strongly stable and the other strongly unstable. It is interesting that the viscosity or dissipation of the material destabilizes the model. Analogous conclusions have been reached for similar theoretical models elsewhere[3] though the physical significance of this result is still an open question.

Comparison with Probstein-Gold Results

Recall that in Ref. 1 the authors assumed that the flutter frequency was zero (based upon experimental observations). Hence, their approach apparently was to set $\Omega_R = 0$, vary Ω_I and compute values of ε, λ from the equality of real and imaginary parts of Eq. (7) for various selected M. A particular example presented in Ref. 1 was $M^2 = 1.2$ For $\Omega_R = 0$, $M^2 = 1.2$ we find from the present analysis

$$X_0 = M = 1.1; \quad \lambda = 0.38; \quad \text{and thus,} \quad -X_1/i = 0.32$$

In Fig. 3 results from the present analysis and that of Ref. 1 are compared. It is seen the results are in good agreement for small Ω_I and ε^*. From Eq. (8) we see that we are really expanding in terms of $X\varepsilon$ and therefore X or Ω should not be too large for our expansion to be accurate. A representative numerical value of ε^* may be obtained using the data of Ref. 4 and 5. From Ref. 4

$$M = 2.55; \quad c_f = 0.0026; \quad \mu = 14.5 \text{ poise}; \quad 2\pi/\alpha = \lambda = 0.3 \text{ cm}$$

From Ref. 5

$$G = 4500\text{–}9000 \text{ psi}$$

and hence, $\varepsilon^* \sim 10^{-3}$. One may also use the preceding information to estimate

$$\rho_f U_f^2 \sim 10 \text{ psi}$$

These estimates are very approximate since we have used the data of Ref. 4 for a liquid layer and the data of Ref. 5 for Teflon at room temperature. But they should serve as rough guides. In the aforementioned, we have used the definitions

$$\tau \equiv \mu\kappa; \quad \kappa \equiv \tfrac{2}{5}(\gamma M^2/2G)c_f$$

Conclusions

In previous work on related problems[2] it has been found that the "practical" stability boundary is generally the strong instability found at coalescence, in the present example as $\lambda \to \frac{1}{2}$. Moreover the finite dimensions of the problem and the precise nature of the material elasticity and dissipation have been found to be important at supersonic conditions[6] though less important at subsonic Mach numbers. This suggests that the present model may need certain refinements. For example, one or more of the finite dimensions of the solid may be important or, as suggested by Nachtsheim,[7] the inner solid is really a thin liquid film which generates its own characteristic scale length.

Also we may take the opportunity to evaluate approximations to the high-speed gas flow which have been used by some investigators.[7] These are:

Quasi-steady theory ($\omega/U\alpha \ll 1$)

$$p = e^{\pm i\alpha(M^2-1)^{1/2}y} \tag{4}$$

$$\lambda X^2/[i\varepsilon X+1] = (M^2-1)^{1/2} \tag{8}_{qs}$$

or

Piston Theory $M(1+\omega/U\alpha) \gg 1$

$$p = e^{\pm i\alpha(M+\omega/U\alpha)} \tag{4}$$

$$\lambda X^2/(i\varepsilon X+1) = X \tag{8}_{pt}$$

From Eq. $(8)_{qs}$, solving for X, one concludes the model is always stable. From Eq. $(8)_{pt}$, one obtains

$$X = (\lambda+i\varepsilon)/(\lambda^2+\varepsilon^2) \simeq 1/\lambda + i(\varepsilon/\lambda^2) \quad \text{for} \quad \varepsilon \ll \lambda$$

This latter result is a reasonable approximation to the stable pole as shown in Fig. 2. However, neither of these approximations will give any useful information concerning the unstable pole and, therefore, must be considered inadequate for the present model. Finally we note that Gold, Probstein, and Scullen[5] have recently treated the shear flow velocity profile flow and also considered alternative surface models. Additional such studies would appear warranted particularly with regard to characterizing the surface more accurately. Shear flow effects have also been treated recently in the context of another though similar problem.[8]

References

[1] Probstein, R. F. and Gold, H., "Cross-Hatching: A Material Response Phenomena," *AIAA Journal*, Vol. 8, No. 2, Feb. 1970, pp. 364–366.

[2] Dowell, E. H., "The Flutter of Infinitely Long Plates and Shells," *AIAA Journal*, Vol. 4, No. 8, Aug. 1966, pp. 1307–1318.

[3] Dugundji, J., Dowell, E. H. and Perkin, B., "Subsonic Flutter of Panels on Continuous Elastic Foundations," *AIAA Journal*, Vol. 1, No. 5, May 1963, pp. 1146–1154.

[4] Nachtsheim, P. R. and Hagen, J. R., "Observations of Cross-Hatched Wave Patterns in Liquid Films," AIAA Paper 71-622, Palo Alto, Calif., 1971.

[5] Gold, H., Probstein, R. F. and Scullen, R. S., "Inelastic Deformation and Cross-Hatching," *AIAA Journal*, Vol. 9, No. 10, Oct. 1971, pp. 1904–1910.

[6] Dowell, E. H. and Ventres, C. S., "Flutter of Low Aspect Ratio Plates," *AIAA Journal*, Vol. 8, No. 6, June 1970, pp. 1162–1164.

[7] Nachtsheim, P. R., "Stability of Cross-Hatched Wave Patterns in Thin Liquid Films Adjacent to Supersonic Streams," *The Physics of Fluids*, Vol. 13, No. 10, Oct. 1970, pp. 2432–2447.

[8] Dowell, E. H., "Generalized Aerodynamic Forces on a Flexible Plate Undergoing Transient Motion in a Shear Flow with an Application to Panel Flutter," *AIAA Journal*, Vol. 9, No. 5, May 1971, pp. 834–841.

Study of 8–15 km/sec Shock Waves Using Conventional Shock Tubes

J.-C. LEBOUCHER* AND M. PINEGRE*

Commissariat à L'Énergie Atomique, Sevran, France

AND

P. VALENTIN†

Université de Rouen, France

IT has been demonstrated[1] that it is possible to increase the shock wave velocity, for a given over-all pressure ratio P_{40}, by dividing this ratio among one or several intermediate chambers. We have studied and operated a shock tube with one so-called middle pressure chamber. The velocity gain g of that tube, compared to the one-diaphragm apparatus, becomes noticeable when P_{40} exceeds 10^5 and when the pressure P_1 of the light gas (H_2 or He) in the intermediate chamber has an optimum value. This gain is approximately 40% when $P_{40} = 10^7$.

The main characteristics of our double diaphragm shock tube are: the combustion of an O_2—H_2—He homogeneous mixture (molar proportions 1-2-7) takes place in the high-pressure chamber, HP (length $L = 0.5$ m; diam $\phi_{int} = 150$ mm), and enables conditions there to reach a few kilobars and 2500°K within a few milliseconds. The middle pressure chamber, MP ($L = 2$ m; $\phi_{int} = 100$ mm), is filled up with H_2. The low-pressure chamber, BP ($L = 12$ m; $\phi_{int} = 100$ mm), is made of stainless steel. The diaphragm D_1 which separates HP and MP chambers is made of stainless steel and scribed on two perpendicular diameters. The diaphragm D_2 between MP and BP chambers is made of thin mylar. One assumes that it opens instantaneously and does not disturb the flow. Some experiments with argon under 0.1 torr show that the shock velocity exceeds 14 km/sec.

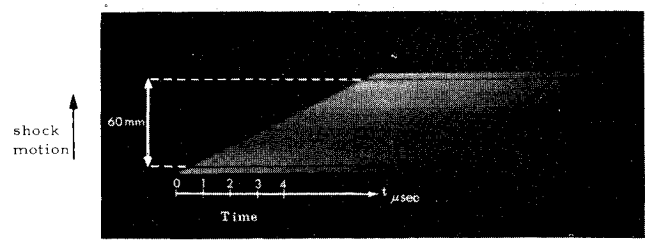

a) Continuous writing streak camera 7 m from second diaphragm— $U = 9.4$ mm/μsec

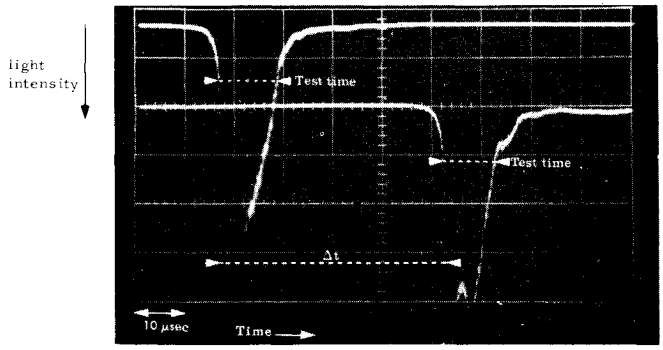

b) Photomultiplier oscillograms: PM are located 9.8 and 10.2 m, respectively, from second diaphragm $U = 400/\Delta t = 9.0$ mm/μsec, test time $\simeq 10$μsec

Fig. 1 Shock wave velocity and test time for initial argon pressure $P_0 = 1$ torr.

Received October 27, 1971; revision received December 30, 1971.

* Ingénieur.

† Professeur, Ingénieur-Conseil au C.E.A.

Index categories: Supersonic and Hypersonic Flow; Shock Waves and Detonations; Research Facilities and Instrumentation.